

Measuring the Galactic Rotation Curve using the 21cm Hydrogen Line

Cameron Cackett
KCL Undergraduate
(supervised by Dr. Jeff Grube)

April 2023

Abstract

We will explore the work done to improve the King's Radio Telescope and highlight the importance of the neutral hydrogen line for studying the structure and dynamics of our galaxy. We also discuss the challenges involved in conducting radio observations of the Milky Way and why we chose to use SALSA telescopes. We present our results, measuring the rotation curve of the galaxy, which shows a relatively constant velocity distribution that deviates from the Keplerian prediction, in agreement with other measurements in the field. This discrepancy provides evidence for the existence of a dark matter halo in the Milky Way.

Contents

1 Radio Astronomy	3
2 The 21 cm Hydrogen Line	3
3 King's Radio Telescope	4
3.1 Primary Dish	5
3.2 Antenna and Dish Feed	5
3.3 Electronics	5
3.3.1 Low-Noise Amplifier	5
3.3.2 Software Defined Radio Receiver	6
3.4 Software	6
3.5 Operation	7
3.6 Issues with the KRT	7
3.6.1 Location and Interference	7
3.6.2 Faulty Equipment	7
4 SALSA	8
5 The Rotation Curve of the Milky Way	9
5.1 Rotation Curve Prediction	9
5.2 Interpreting Observations	9
5.3 Defining Galactic Position	10
5.4 Plotting a Rotation Curve	10
5.5 The Code	11
6 Results	12
7 Rotation Curve or Line?	12
7.1 Difference from Predictions	12
7.2 Sources of Error	12
8 Conclusions	14
A Appendix - Code	17
B Appendix - Graphs	21

1 Radio Astronomy

A difficulty in astronomy with the use of visible light is that observations are often obscured. Objects of interest can remain unseen, hidden behind interstellar gas clouds, making the study of our own galactic structure difficult. Larger wavelengths, such as radio waves, are however able to travel greater distances without absorption and have the ability to penetrate Earth's atmosphere. There are a wide range of different radiation sources which we can detect, radio waves are electromagnetic waves with a frequency between 3Hz and 3THz [ITU, 1995]. Because of this radio astronomy has many uses to scientists, especially with the various radio sources observable to us including stars, galaxies and background radiation.

Radio telescopes are generally considered less approachable to amateurs than optical astronomy, and there are numerous reasons for this. One reason for the difficulty is cost - an amateur approach to radio astronomy requires either spending lots of money or being prepared to build it yourself. There are a wide range of resources online that can aide in the construction of a radio telescope but it still requires a large background knowledge. Another reason is the skill gap - you do not need a lot of expertise to point a basic optical telescope and observe the moon, interesting observations with radiowaves however are less well known. Also the resolution of radio astronomy hurts its appeal to amateurs, having no eyepiece and imaging a 1 pixel resolution is not as visually interesting.

There are upsides to radio astronomy over optical observations. The scattering of sunlight by atmospheric gas molecules and dust particles at visible and ultraviolet wavelengths, known as Rayleigh scattering, causes a bright daytime sky, making it difficult to observe faint objects optically. However, radio wavelengths are much longer than atmospheric particles, meaning they do not scatter. Resulting in a dark radio sky, many radio observations can be conducted during both day and night as well as cloudy weather [Condon and Ransom, 2016].

Galactic radio sources were first observed in 1932 by Karl Jansky, an engineer at Bell Laboratories, who was tracking the source of noise

affecting short-wave transatlantic radio communications. After discovering the noise source followed the stars in the night sky, Jansky shared his findings with an astronomer who concluded the source of this noise was galactic dust clouds [NRAO, nd]. Building on Jansky's work, many discoveries were made utilising radio astronomy such as Jocelyn Bell's discovery of pulsars in 1967. Bell observed a repeating radio pulse every couple of seconds, the object was a pulsar and was originally named LGM-1 (or little green men, jokingly referring to the extra terrestrial nature) [Hewish et al., 1979]. Despite finding the initial radio signal Bell did not receive the Nobel Prize along with her supervisor as she was a PhD student at the time.

2 The 21 cm Hydrogen Line

A neutral hydrogen atom consists of a single proton and electron, even when the electron is in the ground state there are two different energy levels it can occupy. The electron and proton pair can either be spin parallel or anti-parallel. There is a slight energy difference between the two states as the parallel pair are less tightly bound having greater energy. The energy difference within this hyperfine structure is minute compared with the energy difference between the ground and first state. The transition between these parallel and anti-parallel states, a spin-flip, releases a photon of energy, $\Delta E = 5.9 \times 10^{-6} eV = 9.5 \times 10^{-25} J$. The wavelength λ of a photon can be calculated using the following equation:

$$\lambda = \frac{1}{\nu} \cdot c = \frac{h}{E} \cdot c \quad (1)$$

where ν is the frequency of the wave, c is the speed of light, h is Planck's constant, and E is the energy of the wave.

Using the energy difference of the hydrogen line, the wavelength of the wave can be calculated to be about 21cm and the corresponding frequency is 1420MHz. Although we know that hydrogen is the most abundant element in the universe, there are not as many of these signals as implied. With a transition rate of $3 \times 10^{-15} s^{-1}$ and a mean lifetime within the excited state of 10 million years, the effects of the abundance of the element balance with the rarity of the transition [Wiese and Fuhr, 2009].

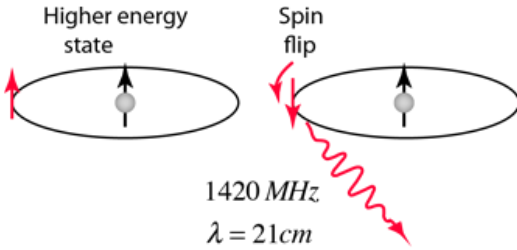


Figure 1: Spin flip of an electron in a hydrogen atom. On the left nuclear spin and electron spin are parallel, whereas on the right they are antiparallel. The flip results in a 21cm radio wave being emitted.[Hyperphysics, 2000]

The existence of the 21cm hydrogen line was first predicted in 1945, by Hendrik van de Hulst, and later observed by Edward Purcell and Harold Ewen at Harvard in 1951. These discoveries were made around the beginning of radio astronomy and led to the first mapping of neutral hydrogen in the Milky Way in the 1950s. In 1959 at Geneva, the International Telecommunication Union declared the frequency range of 1400MHz – 1427MHz as protected for astronomical use [Smith-Rose, 1962]. More modern uses of hydrogen line observation include cosmology, and the search for extraterrestrial intelligence (SETI). In Cosmology, observations of redshifting of the 21cm line allows study into the early universe.

New, advanced telescopes are being used to learn about early star formation and the thermal history of the universe [Pritchard and Loeb, 2012]. In 1959 Giuseppe Cocconi and Philip Morrison from Cornell University discussed how two civilisations would approach interstellar communication. Radio waves would be a clear choice over shorter length radiation due to its ability to travel long distances without absorption. A range of 1GHz – 10GHz was deemed best, at greater frequencies our atmosphere and perhaps those of other planets emit radiation, at lesser frequencies there is a loud background from our galaxy. The 21cm hydrogen line (1.42GHz) happens to sit within this 'Microwave Window', due to its importance an advanced civilisation will likely be observing at this frequency, making it a likely candidate for interstellar communications to be sent [SETI, nd].

3 King's Radio Telescope

The King's Radio Telescope (KRT) is a project aiming to build a 2.4m radio telescope capable of detecting 21cm radiowaves and observing neutral hydrogen in our galaxy. In 2020 the components were purchased from RF HAMDESIGN, however as a result of the Covid-19 pandemic, the first group was not able to start ground work on the antenna until 2022. Over the course of the semester they set up the dish, measured the focal length of the telescope, and began testing the electronics. Unfortunately there were too many tasks for the telescope to become operational that year.



Figure 2: Last year's group assembling the dish.

This report follows the second group working a year later on modifications to the electrical equipment and software in an attempt to collect the first results.



Figure 3: Project members holding up the telescope: (from left to right) Ana Pilar Ravané, Katie Robertson, Muhammad Ibrahim, Maksymilian Ogorzalek, and myself.

3.1 Primary Dish

The telescope features a parabolic dish with diameter of 2.4m, the dish is built around an aluminium disk with twelve struts and four concentric metal rings (as seen in figure 2). Wire mesh is attached to the dish structure to create the reflecting face of the telescope. We are able to use a mesh dish as the wavelength of the incoming radiowaves are much longer than the size of the gaps in the mesh. The primary dish is analogous to the primary mirror of a reflecting telescope. The assembling of the primary dish can be seen in figure 2.

3.2 Antenna and Dish Feed

The dish feed is a small orange cylindrical case that sits at the focal point of the telescope. The internal facing side of the dish feed is made from a thin plastic allowing radio waves to enter, the other side of the dish feed is a metal plate that serves as a secondary reflector for radio waves. The dish feed is held at the focal point of the primary dish by three metal rods and a metal holder shown in figure 3. The telescope was designed and built with a focal length over diameter ratio (F/D) of 0.45. With a diameter of 2.4m this means the dish feed must be placed at 1.08m from the centre of the dish [RF-HAMDESIGN, nd].

Our antenna is a loop antenna which is a small metal loop sitting inside the dish feed, connected via a coax cable to the electronics. The length of the wire determines its resonant frequency, this is the frequency at which the By matching the length to the desired wavelength we can ensure the telescope is optimized for detecting the 21cm hydrogen line.

3.3 Electronics

The antenna outputs an electronic signal which first needs to be amplified before then being digitized and sent to a laptop to record. This is done using various electronic components, first the signal is carried by a coax cable to the low-noise amplifier (LNA). This cable is kept short as it has greater risk of picking up noise over distance than later when the signal is transported digitally. After the signal is amplified it is sent to the software defined radio (SDR) receiver, where it is

converted to a digital signal and sent via USB to a laptop.



Figure 4: Our electronic setup inside a copper coated box.

An initiative we took to reduce the noise in our data was building a box to house our electronics. The electronics had to be near the antenna to avoid the need for a long coax cable which could be a source of noise. This meant however that radiation from the electronics could be picked up by the telescope adding noise to the results. The box was made of cardboard but coated in copper tape which absorbs radiowaves preventing radiation from the electronics affecting the data. We also designed the box to be placed on top of the dish feed which allowed us to connect our electronics straight to the antenna. We only needed a small adaptor replacing the coax cable and removing another potential noise source.

3.3.1 Low-Noise Amplifier

As the signals we are searching for are relatively faint it can be difficult to separate signals from noise. To reduce the impact of noise on our data an LNA is used amplify the incoming signal while adding as little noise as possible. This is otherwise known as increasing the gain, the amplification of the signal received over the signal that an ideal noiseless telescope would receive. Gain is usually measured in decibels (dB), a logarithmic scale used to measure sound. A gain of 30dB would mean that the signal received is being amplified a magnitude of a thousand. The hope with using an LNA is that the quality of the data can be improved by limiting uncertainty due to noise. The LNA we used was a SAWbird (figure

5), specifically designed for amplifying 21cm hydrogen observations. This LNA takes in the electrical signal amplifies it and outputs on the other side. It can be powered through the receiver from the laptop via USB, or it can be powered by a separate micro USB port [PhysicsOpenLab, 2020b].



Figure 5: Nooelec SAWbird + H1 [Nooelec, 2019]

Attempts at using one LNA had produced data with a high amount of noise, any signal being detected was too weak to differentiate and more gain was needed. To rectify this we decided to use two LNAs, this greatly increased the gain, and allowed us to first witness a possible 21cm signal. It did present a problem with power as the 5V USB output is only able to power one LNA. This meant that the other LNA had to be powered by a portable power bank. A DC current blocker was used in between the two LNAs to ensure neither LNA receives too many volts, causing damage.

3.3.2 Software Defined Radio Receiver

Software defined radio is the modern alternative to traditional options such as superheterodyne receivers. The signal is processed digitally rather than utilizing lots of hardware. There are numerous advantages to using an SDR receiver over an analog one such as: being able to isolate weak signals from noisy backgrounds, the cost efficiency of not having to buy lots of analog equipment, and the simplification of parts meaning there are less opportunities for error. A downside to SDR receivers is they are usually set to a limited frequency range, though this is not a problem for us as our receiver is designed for the specific frequency we are observing [Pandian B et al., 2022].



Figure 6: Our chosen SDR receiver was the Airspy Mini. It is compact with an electronic input and digital output via USB. [Airspy, nd]

3.4 Software

One of the first things our group identified as a priority for our project was the need for new software. The previous group had encountered difficulties with their software, so we decided to explore other options. After some research, we opted for the gr-radio_astro package, which is part of the DSPiRA project at the University of West Virginia. This package is designed to help students and enthusiasts get into radio astronomy using GNURadio, a free open-source software development toolkit that enables users to process their data with a wide range of signal processing blocks [Supriyatno et al., 2015]. To ensure accessibility, I installed GNURadio and the gr-radio_astro package onto a bootable USB flash drive, enabling anyone to run the software without the need for installation on their laptop.

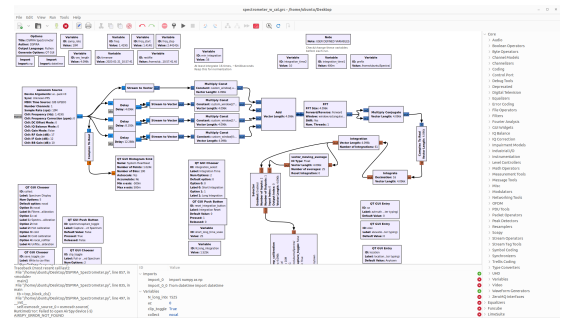


Figure 7: Screenshot of the GNURadio GUI with the gr-radio_astro package installed.

The screenshot in figure 7 shows various signal processing blocks, the first of which being the osmocomm Source block which acts as the interface for the airspy. The first step in signal processing is the polyphase filter which separates a wideband radio signal into multiple narrowband

channels, allowing more efficient processing. The following steps are a Fourier transform, multiply conjugate which takes the square modulus (determines signal strength at each frequency), and then integration. Integration time is an important setting, the more time the data is integrated over the less the effect of random noise spikes but the the data will take longer to collect. The next step is the system temperature calibration which calibrates the results, outputting the spectrum, gain and system temperature. Finally this data is sent to their respective GUI Vector Sinks for display in the graphical interface [PhysicsOpenLab, 2020a].

3.5 Operation

Before data can be collected the software needs a baseline to compare to, requiring a hot and cold calibration. The hot calibration is carried out first and involves pointing the telescope at known source of radiation, with a known stable flux density. The signal from this source is measured by the receiver and used to determine the gain and sensitivity of the system. Next the cold calibration involves pointing the telescope at a region of the sky known to have little radio sources, this helps the receiver set a baseline and is used to determine system temperature and noise level [West Virginia University, 2020].

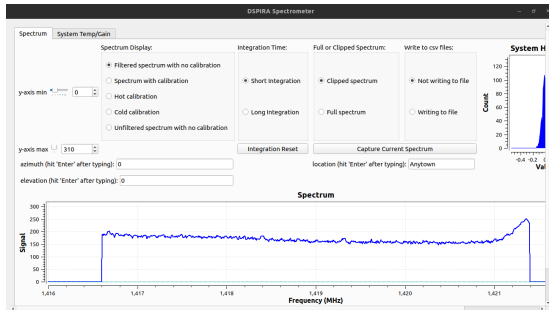


Figure 8: Screenshot of the output GUI with with an uncalibrated spectrum.

It is important to understand how important parameters are calculated:

$$G = \frac{P_{hot} - P_{cold}}{T_{hot} - T_{cold}} \quad (2)$$

$$T_{system} = \frac{T_{hot} - T_{cold}(P_{hot}/P_{cold})}{(P_{hot}/P_{cold}) - 1} \quad (3)$$

$$T_{object} = \frac{P_{measured}}{G - T_{system}} \quad (4)$$

where G is the gain, T is the temperature and P is the signal intensity [PhysicsOpenLab, 2020a]. Hot and cold calibrations can be carried out by switching to the 'Spectrum Display', as shown in figure 8, and then switching to 'Spectrum with calibration' to display the calibrated data. To record results, 'Writing to file' must be enabled. It should also be noted that there are two integration time settings, which allow for quick switching between 0.4s and 10s integration times (these can be adjusted in the variable boxes in figure 7). The resulting data is saved as CSV files on the flash drive.

3.6 Issues with the KRT

Ultimately despite our best efforts over the ten week period we were unable to get the KRT operational such that we were confident with its output. We managed to decrease its noise and increase its gain but unfortunately we did not manage to get a strong 21cm observation. The addition of the second LNA and the assembling of the copper box did assist in reducing noise, but there were other issues.

3.6.1 Location and Interference

One problem we encountered was location, the telescope is housed in the Boat House in King's College London and we do not have the ability to transport it elsewhere. This can be a problem as the Strand, Central London is not an ideal location for radio astronomy due to the abundance of noise sources. Cities in general struggle with radio interference and, despite our desired frequency being in a protected band for astronomy, there is no guarantee against interference from the spillover of overly-broad transmitters. Also unintentional radiation from electronic devices was hard to avoid, especially in a busy public areas. Another issue with the location was the surroundings and time of year. The telescope could not be used before midday due to the galaxy passing behind tall buildings, limiting the time we could collect data.

3.6.2 Faulty Equipment

Ideally the telescope would be mounted on a tripod and controlled remotely by a motor. Unfortunately despite having a working motor and tripod our remote control was not functional. It

had to be sent back to the Netherlands for repair and by the time we received it back we had run out of time to use the telescope. We did not let this stop us from testing the telescope, instead we needed three people to hold the telescope and one person to monitor the output on the laptop. The motor controller would have allowed us to set our desired altitude and azimuth angles, instead we used the stellarium app on our phones to measure the angle our telescope was pointing at. This introduces a lot of uncertainty with the accuracy of our phones compass and our ability to hold the heavy telescope steady.

There was a second issue we encountered with the equipment from RF HAMDESIGN - our antenna. For a while we were only detecting noise and could not pick up a signal, and after exhausting other options we decided to cut open the dish feed and discovered our antenna was broken. This would explain our struggle in finding a signal at the resonant frequency of the antenna. It was a simple fix to reattach the antenna but unfortunately the problem was discovered in week nine of ten, limiting our time to collect data.



Figure 9: A closeup on the opened dish feed with the broken loop antenna.

The final issue preventing us from collecting data from the KRT was its structural stability. The dish feed is attached to the primary dish by the three struts and a metal holder. Unfortunately one of the three connectors between the strut and dish feed began to thread, and as we used the telescope the instability only increased. This lead to dramatic changes in noise and signal as the direction the antenna was facing changed as the telescope moved. The telescope only works at its best when the dish feed is aligned with the centre of the primary dish, any instability in the

structure severely affects the ability to collect results.

4 SALSA

Determined not to let the problems with our own telescope affect our investigation we searched for another way to collect data, this was when we discovered SALSA. "Such a lovely small antenna" is actually a set of three 2.3m radio telescopes based at Onsala Space Observatory in Sweden. Anyone can book time slots to control these telescopes for free, supported by the European Hands-On Universe project. After booking a session the telescope can be accessed via a browser, the interface allows the tracking of satellites or pointing at specific coordinates. The integration time of the telescope can also be controlled as shown in figure 10.

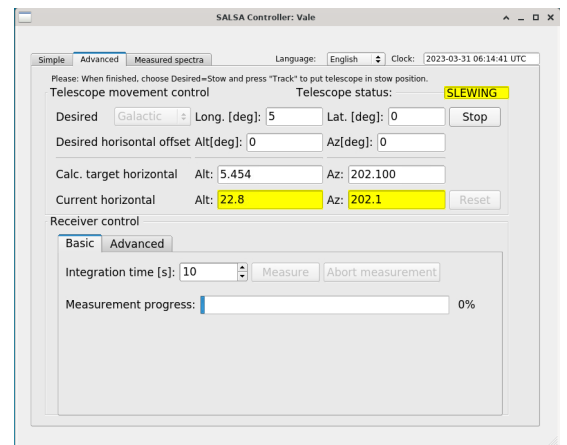


Figure 10: The SALSA remote control interface, set to desired galactic coordinates and an integration time of ten seconds.

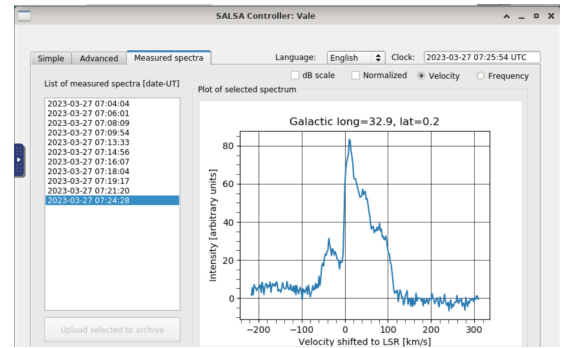


Figure 11: An example of a measured spectra from the Vale telescope.

Exported data is saved on your SALSA account and can be downloaded as a graph or the raw data in a text file from the data archive. There is also a live webcam feed of two of the

small telescopes, so you can watch as you remotely control it.



Figure 12: Webcam view of Vale and Brage telescope. The larger radio telescope on the right is a part of Onsala Space Observatory.

The SALSA telescopes have a tracking accuracy of 0.5° , meaning that we are only able to select coordinates to the nearest 1° . This is not a problem however as 1° is relatively small compared to the angular size of the telescope beam which is 6° . The telescope is also limited to a minimum altitude for observing due to its surroundings of 15° . This is helpful as altitudes close to the horizon risk more interference from Earth's radio signal emission, but also means we are unlikely to observe longitudes close to 0° at any time [Horellou et al., 2018].

5 The Rotation Curve of the Milky Way

5.1 Rotation Curve Prediction

A rotation curve is a plot of the orbital velocities of objects in the galaxy compared their distance from the galactic centre. Assuming that the stars and gas clouds orbit in a circular path and using Newtonian mechanics we know the orbital velocity (ν) of an object is given by [Sofue, 2013]:

$$\nu \approx \sqrt{\frac{GM}{R}} \propto \frac{1}{R} \quad (5)$$

This implies that the further from the galactic centre the slower objects should be travelling and is known as a Keplerian velocity curve. This proves true for the solar system, the planets roughly follow this relation as shown in figure 13.

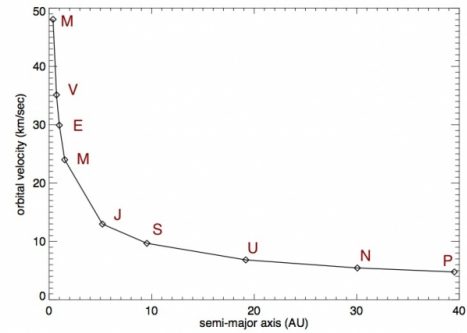


Figure 13: Velocity rotation curve of the planets in our solar system.[Palma, nd]

5.2 Interpreting Observations

If neutral hydrogen is present across the universe, why observe it? The objective is not just to determine the presence of interstellar gas clouds, but to understand more about the structures around us. The Milky Way, like other spiral and barred spiral galaxies, has large arms containing an abundance of interstellar hydrogen. Photons from the hydrogen line will not be observed at the exact same frequency they were emitted. This is due to the relative velocity of the gas compared with us as the observer and the Doppler effect. The Doppler effect is a phenomenon which can be observed in everyday life, the horn of a car travelling towards you will have a higher pitch/frequency than a car travelling away. This is because the waves are emitted with the same speed in every direction from the source, but if the source has velocity relative to the observer, then the waves appear compressed in the direction of travel of the source. The same applies to electromagnetic waves, observations of an distancing source will appear to have a lower frequency and longer wavelength than a stationary one - this is known as redshift. An approaching source will appear as a higher frequency and shorter wavelength, known as blueshift.

This is advantageous as it allows us to determine the velocity of the gas by measuring the degree to which the frequency has shifted. The degree to which an object is redshifted can be calculated using the following equation [Huchra, nd]:

$$z = \frac{\lambda_0 - \lambda_e}{\lambda_e} \approx \frac{\nu}{c} \quad (6)$$

where λ_0 and λ_e are the observed and emitted wavelengths, vis the relative velocity to the

observer. The approximation relies on non-relativistic velocities ($v \ll c$). Given this condition the relative velocity can be calculated by the following:

$$\nu = \frac{(\lambda_0 - \lambda_e)c}{\lambda_e} \quad (7)$$

5.3 Defining Galactic Position

The difficulty with finding the position of objects within the Milky Way is that we are inside of it. It is much easier to make observations of nearby galaxies and determine their shape and structure. A simple measurement such as the distance to our galactic centre (R_0) remains uncertain. Estimates from the last two decades suggest a R_0 value of between 7.4 – 8.7 kiloparsecs [Abuter et al., 2019]. This is relatively uncertain when compared with distances to further objects such as other galaxies.

It is also important to note how we define an objects position in the galaxy. With both the Earth's rotation and orbit affecting the position of objects in our sky, we rely on galactic coordinates to locate objects in the Milky Way. The gal. coord. system works as a spherical system with the Sun at the centre, the galaxy is roughly a flat plane corresponding to a latitude of around 0° . For simplicity we can then focus just on galactic longitude which is split into four quadrants as shown in figure 14.

5.4 Plotting a Rotation Curve

With the aim of plotting a rotation curve, the distance to the observed gas clouds is very important. Using optical light we are only able to observe the closest gas cloud as any other clouds behind would be obscured. This is an advantage of using the 21cm line as multiple gas clouds in the same direction will appear with different wavelengths provided they are travelling at different relative velocities. Analysing the different shifted wavelengths will only explain how many gas clouds we are observing and how fast they are moving, but not how far away they are. A technique is needed to take this information and calculate the distance. This is where the tangent method is used, by assuming our line of sight on \mathbf{M} is tangential to the orbit of \mathbf{M} , we can calcu-

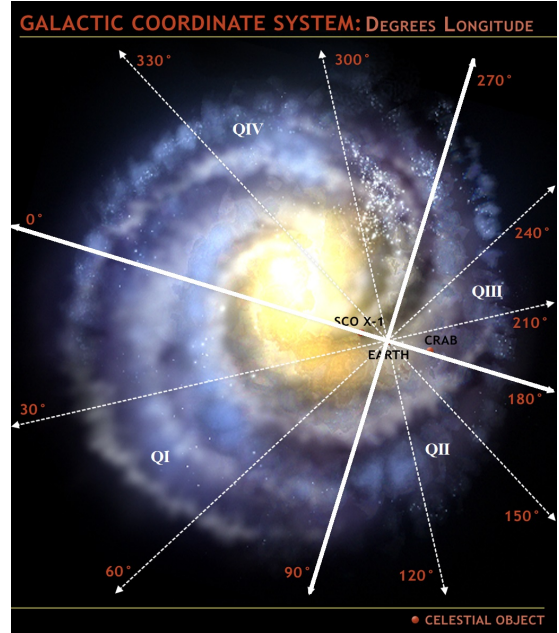


Figure 14: An artist's impression of the Milky Way showing galactic longitude. The solar system is at the centre, and galaxy is split into four quadrants. QI: 0° – 90° , QII: 90° – 180° , QIII: 180° – 270° , QIV: 270° – 360° . [UoA, nd]

late the distance to \mathbf{M} using its relative velocity to us, as seen in figure 15.

Using angles from figure 15 and trigonometry we can create an equation for the relative velocity (V_r):

$$V_r = V \cos \alpha - V_0 \cos \beta \quad (8)$$

where V is the velocity of object \mathbf{M} , and V_0 is the velocity of the sun. For calculations in this report we will use these values: velocity of the Sun $V_0 = 220 \text{ km s}^{-1}$ and the radius of the Sun's orbit $R_0 = 8.5 \text{ kpc}$. Looking at the diagram and knowing that the angles of a triangle sum to 180° we can calculate that $\alpha = a$ and $\beta = l$. Also using trigonometry we can work out that $\cos a = \frac{R_0 \sin l}{R}$. By substituting this information into equation 8 we get:

$$V_r = V \frac{R_0}{R} \sin l - V_0 \sin l \quad (9)$$

With this equation we could use any longitude however to help ensure our observations are focused within the solar orbit we are observing quadrant I [Liu, 2008].

Looking back at the spectrum in figure 11 we see multiple peaks, so which do we use to calculate velocity? The spectrum has multiple peaks as there are multiple overlaying signals. In this example the telescope is pointed in the direction of multiple gas clouds at different distances. We

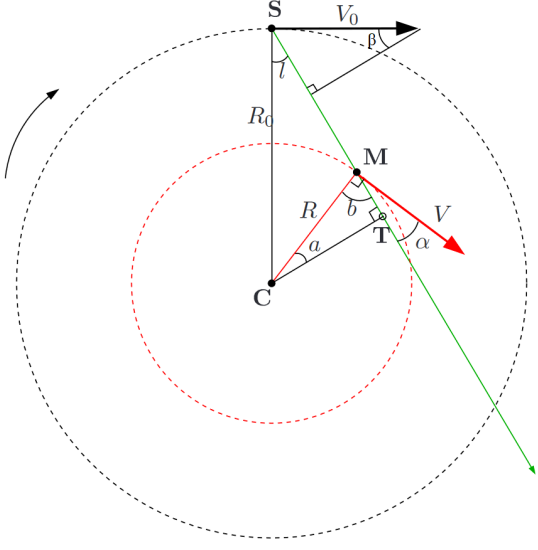


Figure 15: The geometry of our galaxy, where **S** represents the Sun, **M** represents the gas cloud being observed, and **C** represents the centre of the galaxy. The green line from **S** to **M** is the line of sight and l is the gal. long.

[Horellou et al., 2015]

could try to separate and analyse each peak but to use the tangent method we require the observed gas clouds to be within the solar orbit. Galactic clouds at the same or greater distance from the galactic centre compared to our Sun will travel at the same orbital velocity or slower. This means we can ignore the slower peaks. We also choose to record the peak with the greatest relative velocity ($V_{r,\max}$) as the velocity of this gas cloud will be most aligned with the line of sight increasing the accuracy of the tangent method.

A gas cloud at the tangent point (**T**) will have an orbital radius [Chemin et al., 2015]:

$$R = R_0 \sin l \quad (10)$$

Putting this into equation 9 gives [Liu, 2008]:

$$V = V_{r,\max} + V_0 \sin l \quad (11)$$

Therefore by knowing orbital velocity and orbital radius of the sun, the galactic longitude observed, and the greatest relative velocity we can plot the distance and velocity of gas clouds in our galaxy.

5.5 The Code

The code was another aspect of the project that piqued my interest, and I took the initiative to develop a Python notebook (Appendix A) that processes raw data from SALSA and generates a rotation curve for the galaxy. The first step in

the code is to load the files and perform basic setup (Listing 1). Next, the files are renamed to their galactic coordinates (Listing 2). This is accomplished by opening each text file, reading it, storing the galactic coordinates, and then renaming the file to the rounded galactic coordinates before closing it. By doing so, we don't have to read the entire file again to access the coordinates. Instead, we can simply read the actual data and obtain the galactic coordinates from the file name. Having the galactic coordinates in the file name also facilitates the search for specific data points since the text files are initially named using a generic spectrum_number format. The third step is optional and involves plotting the galactic coordinates of the collected data (Listing 3). This step is useful for identifying any missing data points, which can be easily overlooked when collecting large amounts of data from SALSA.

Next I created a function which plots each data file and determines the peak velocity and max velocity, saving them to an array (Listing 4). It does this by determining positive velocity with the peak intensity, this is not always useful as data may show multiple peaks. To solve this we find the greatest velocity value with an intensity of 90% of the peak, allowing us to select the highest velocity peak or near to. The max is determined by finding the first point after our peak value with an intensity equal to the peak intensity times the threshold. The threshold is set in the last line of this code block within the function parameters (for this report we are using a threshold of 20%). While this system is not perfect in determining our max/peak values, it does a good job at estimating them and saving time. It can process hundreds of data files in the time it would take a person to determine by eye and input the value. Also the max values are not easy to determine even by a human, so using this code allows the process to be easily repeatable by another group.

The final parts of the code were mainly written by our supervisor Dr. Jeff Grube (Listings 5 – 8). It takes the peak and max velocities and plots a rotation curve using equations 10 and 11. The rotation curve is a plot of the calculated velocities compared to their distance to the gal. centre. We also compare our data with those collected by N. M. McClure-Griffiths and J.

M. Dickey [McClure-Griffiths and Dickey, 2007] as well as a model put together by Stacy McGaugh [McGaugh, 2018].

6 Results

Between the hours of 7:00am and 10:30am BST on March 31st I used the Vale telescope to collect spectra at a latitude of 0° and longitudes ranging from 5° to 90° . I also collected results at the same longitudes but with latitudes of $\pm 3^\circ$ and $\pm 6^\circ$, but decided not to include them in this report as the tangent point method assumes we are working in a flat galactic plane (0° latitude). Using the entire data set would provide the same general trend but with greater uncertainty. As the angular size of the antenna beam is about 6° we decided to increase the galactic longitude in steps of 3° as smaller increments would not be noticeable.

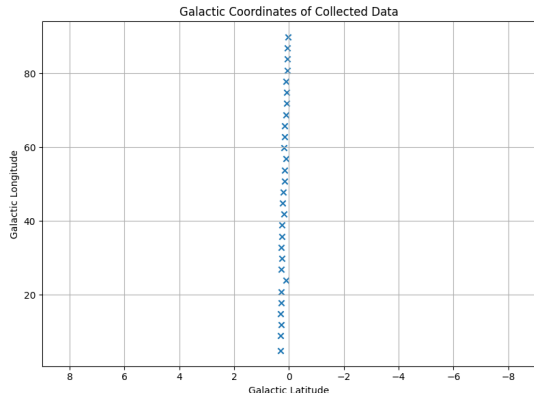


Figure 16: A plot of the data points used. The drift from 0° is explained by the mechanical limit to the tracking of the telescope.

7 Rotation Curve or Line?

The data was then plotted (See Appendix B, figure 16), the peak and max velocity values are calculated and the final rotation curve is plotted (figure 17). The data and model shows a steady velocity, relatively independent from the distance to the galactic centre. This is in contrast to the Keplerian prediction in section 5.1 which suggests objects in our galaxy should orbit slower with greater radius.

Looking at the data collected from Salsa, the max velocity values as expected appear more accurate, following closer to the data from [McClure-Griffiths and Dickey, 2007]. This suggests the large angular width of the telescope

beam and the resultant overlapping peaks did have an adverse effect mostly mitigated by using max values. The max values follow the model line from the solar orbit, 8.5kpc, to about 3kpc when they start to drop. This is likely due to limitations in the accuracy of the code which interprets the spectra struggling, with more refinement to the code it should be possible to bring the values closer to the model line. It will be difficult to replicate the model completely with our equipment as closer to the galactic centre the peaks bunch closer together making it harder to distinguish them from each other.

The peak values seem to show a straight line from the origin. We know this is not accurate as this velocity distribution would be attributed to a solid body rotating, which we know not to be true for the Milky Way. Overall our max velocity values appear accurate for $R > 3\text{kpc}$.

7.1 Difference from Predictions

The predictions based on Kepler's third law suggested that as orbital radius increased, orbital velocity should decrease. Instead our results show that orbital velocity increases slightly for $R > 3\text{kpc}$, the increase is relatively small and some may characterise this as a constant velocity distribution. If the rotation curve is indeed closer to a straight line than the Keplerian prediction of a curve, it suggests that the gravitational potential in the outer regions of the galaxy is dominated by a mass distribution that extends further than the observable matter, such as dark matter. The presence of a dark matter halo would explain the constant velocity line as it would significantly change the mass distribution of our galaxy compared to what we observe.

7.2 Sources of Error

The uncertainty in processing the data has already been discussed and measures were taken to keep this error at a minimum. There are however unavoidable sources of uncertainty such as the orbital velocity and radius of the Sun. Despite numerous investigations there are still a range of possible values. Another source of error is interference, even though SALSA should expect less interference than we did in central London, there is still an expectation of interference which could affect results.

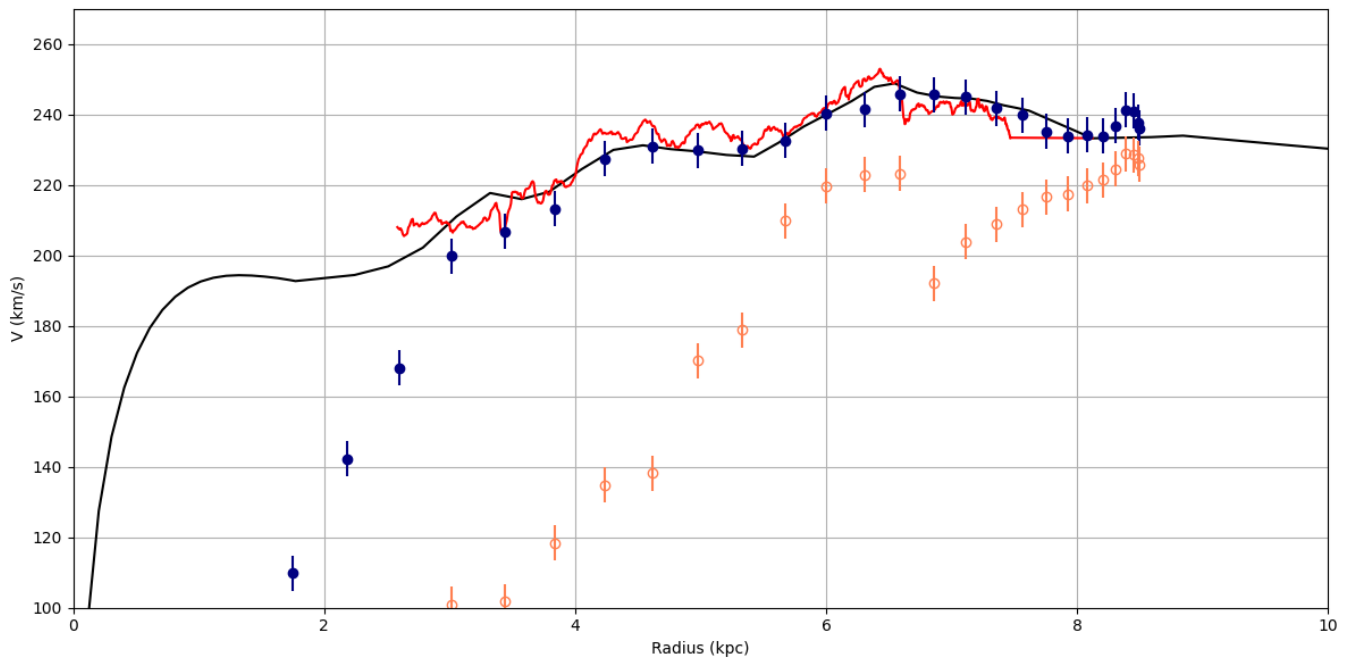


Figure 17: Rotation curve of the Milky Way: the black line is the predicted model from [McGaugh, 2018], the red line follows the data from [McClure-Griffiths and Dickey, 2007], the blue circles are the max velocity values, and the orange (hollow) circles are the peak velocity values.

8 Conclusions

In this report we looked at the importance of the neutral hydrogen line for observations of our galaxy. We also discussed the efforts made to get the King's Radio Telescope operational and why we ultimately decided to use SALSA. We discussed how 21cm observations are interpreted and used to plot rotation curves of the galaxy. Our rotation curve did not match the Keplerian prediction but this is in agreement with the wider community who measure either an increasing or flat velocity distribution. Finally we discussed how this is evidence of a dark matter halo in the Milky Way. Although this report does not reveal new insights to the field it does demonstrate why radio astronomy is critical in the pursuit to understand our galaxy.

References

- [Abuter et al., 2019] Abuter, R., Amorim, A., Bauböck, M., Berger, J., Bonnet, H., Brandner, W., Clénet, Y., Du Foresto, V. C., De Zeeuw, P., Dexter, J., et al. (2019). A geometric distance measurement to the galactic center black hole with 0.3% uncertainty. *Astronomy & Astrophysics*, 625:L10.
- [Airspy, nd] Airspy (n.d.). Airspy mini. <https://airspy.com/airspy-mini/>.
- [Chemin et al., 2015] Chemin, L., Renaud, F., and Soubiran, C. (2015). Incorrect rotation curve of the milky way. *A&A*, 578:A14.
- [Condon and Ransom, 2016] Condon, J. J. and Ransom, S. M. (2016). *Essential Radio Astronomy*. Princeton University Press, sch - school edition edition.
- [Hewish et al., 1979] Hewish, A., Bell, S. J., Pilkington, J. D. H., Scott, P. F., and Collins, R. A. (1979). Observation of a rapidly pulsating radio source. In *A Source Book in Astronomy and Astrophysics, 1900–1975*, pages 498–504. Harvard University Press.
- [Horellou et al., 2015] Horellou, C., Johansson, D., and Varenius, E. (2015). Salsa project documentation: Mapping the milky way.
- [Horellou et al., 2018] Horellou, C., Johansson, D., Varenius, E., and Klopotek, G. (2018). Salsa user manual: Telescope control and data analysis.
- [Huchra, nd] Huchra, J. (n.d.). Extragalactic redshifts. <http://ned.ipac.caltech.edu/help/zdef.html>. Accessed: 21/04/2023.
- [Hyperphysics, 2000] Hyperphysics (2000). The hydrogen 21-cm line. <http://hyperphysics.phy-astr.gsu.edu/hbase/quantum/h21.html>. Accessed: 14/04/2023.
- [ITU, 1995] ITU (1995). Article 1 – terms and definitions. In *Radio Regulations*. International Telecommunication Union.
- [Liu, 2008] Liu, L. (2008). The hydrogen 21-cm line and its applications to radio astrophysics. *Massachusetts Institute of Technology*.
- [McClure-Griffiths and Dickey, 2007] McClure-Griffiths, N. M. and Dickey, J. M. (2007). Milky way kinematics. i. measurements at the subcentral point of the fourth quadrant. *The Astrophysical Journal*, 671(1):427.
- [McGaugh, 2018] McGaugh, S. S. (2018). A precise milky way rotation curve model for an accurate galactocentric distance. *Research Notes of the AAS*, 2(3):156.
- [Nooelec, 2019] Nooelec (2019). *SAWbird+ H1m Low Noise Amplifier (LNA)*.
- [NRAO, nd] NRAO (n.d.). The history of radio astronomy. <https://public.nrao.edu/radio-astronomy/the-history-of-radio-astronomy/>. Accessed: 12/04/2023.
- [Palma, nd] Palma, C. (n.d.). The rotation curve of the milky way. https://www.e-education.psu.edu/astro801/content/18_p8.html. Accessed: 21/04/2023.
- [Pandian B et al., 2022] Pandian B, A., L, G., Inbanathan, S., K B, R., Somashekar, R., and T, P. (2022). Galaxy rotation curve measurements with low cost 21 cm radio telescope.

[PhysicsOpenLab, 2020a] PhysicsOpenLab (2020a). Gnuradio software for the 21 cm neutral-hydrogen line. <https://physicsopenlab.org/2020/07/26/gnuradio-software-for-the-21-cm-neutral-hydrogen-line/>.

[PhysicsOpenLab, 2020b] PhysicsOpenLab (2020b). A low-noise sdr-based receiver for the 21 cm neutral-hydrogen line. <https://physicsopenlab.org/2020/07/26/sdr-based-receiver-for-the-21-cm-neutral-hydrogen-line/>.

[Pritchard and Loeb, 2012] Pritchard, J. R. and Loeb, A. (2012). 21cm cosmology in the 21st century. *Reports on Progress in Physics*.

[RF-HAMDESIGN, nd] RF-HAMDESIGN (n.d.). *Specifications Sheet: PRIME FOCUS MESH DISH KIT 2.4 Meter DISH*. The Netherlands.

[SETI, nd] SETI (n.d.). Seti observations. <https://www.seti.org/seti-institute/project/details/seti-observations>. Accessed: 14/04/2023.

[Smith-Rose, 1962] Smith-Rose, R. L. (1962). The protection of frequencies for radio astronomy. *JOURNAL OF RESEARCH of the National Bureau of Standards*, page 100.

[Sofue, 2013] Sofue, Y. (2013). Rotation Curve and Mass Distribution in the Galactic Center—From Black Hole to Entire Galaxy—. *Publications of the Astronomical Society of Japan*, 65(6).

[Supriyatno et al., 2015] Supriyatno, B. I., Hidayat, T., Susksmono, A. B., and Munir, A. (2015). Development of radio telescope receiver based on gnu radio and usrp. In *2015 1st International Conference on Wireless and Telematics (ICWT)*, pages 1–4.

[UoA, nd] UoA (n.d.). <https://astronomy.ua.edu/undergraduate-program/course-resources-astronomy/lab-exercise-8-cosmic-distributions-and-the-galactic-ecology/1293-2/>. Accessed: 18/04/2023.

[West Virginia University, 2020] West Virginia University (2020). How to calibrate the horn telescope. *Digital Signal Processing in Radio Astronomy*.

[Wiese and Fuhr, 2009] Wiese, W. L. and Fuhr, J. R. (2009). Accurate atomic transition probabilities for hydrogen, helium, and lithium. *Journal of Physical and Chemical Reference Data*, 38(3):565–720.

A Appendix - Code

Processing SALSA 21cm Data.

This Notebook will go through how to process data from SALSA (<https://liv.oso.chalmers.se/salsa/>) and create a rotation curve for the Milky Way. It should be as simple as collecting data from a range of galactic longitudes and putting them into a adjacent folder named 'data'.

Listing 1: The first step is to import relevant modules, as well as general setup.

```
1 import os
2 import matplotlib.pyplot as plt
3 import numpy as np
4
5 plt.rcParams["figure.figsize"] = [7.50, 3.50]
6 plt.rcParams["figure.autolayout"] = True
7
8 fileSM = "processed/salsa_max.txt"
9 fileSP = "processed/salsa_peak.txt"
10
11 with open(fileSM, "w") as f1, open(fileSP, "w") as f2:
12     pass
```

Listing 2: Next we will rename the files with their galactic coordinates.

```
1 #Define the directory path where the files are located
2 directory = 'data'
3
4 #Get a list of all the files in the directory
5 files = os.listdir(directory)
6
7 #Loop through each file
8 for filename in files:
9
10    #Open the file and read the contents
11    with open(os.path.join(directory, filename), 'r') as f:
12        contents = f.readlines()
13
14        #Get the GLON and GLAT values from the file and round to 2 d.p.
15        GLON = round(float(contents[4].strip()[7:]), 2)
16        GLAT = round(float(contents[5].strip()[7:]), 2)
17
18        #Format the GLON and GLAT to be 2 d.p. even if ending with zero.
19        GLON_str = '{:.2f}'.format(GLON).zfill(3)
20        GLAT_str = '{:.2f}'.format(GLAT).zfill(3)
21
22    #Rename the file
23    new_filename = f'{GLON_str}_{GLAT_str}.txt'
24    os.rename(os.path.join(directory, filename), os.path.join(directory,
new_filename))
```

Listing 3: A useful but not required step is to map the galactic coordinates to see what results were collected.

```
1 #Script to plot galactic coordinates of collected data from SALSA
2      telescope.
3
4 directory = 'data'
5 #Name of main folder.
```

```

5
6 files = os.listdir(directory)
7 #Create a list of files.
8
9 xCoords = []
10 yCoords = []
11 #Empty list of coordinates.
12
13 for f in files:
14     spectrum = os.path.join(directory, f)
15     #Attach directory to file names
16     spectrumOpen = open(spectrum)
17     #Open files
18     content = spectrumOpen.readlines()
19     #Read files
20     yCoords.append(float(content[4].replace('#_GLON=','').strip()))
21     xCoords.append(float(content[5].replace('#_GLAT=','').strip()))
22     #Takes number from each coordinate line and adds to list.
23     spectrumOpen.close()
24
25 plt.scatter(xCoords, yCoords, marker="x")
26 plt.title('Galactic Coordinates of Collected Data')
27 plt.ylabel('Galactic Longitude')
28 plt.xlabel('Galactic Latitude')
29 plt.ylim(9, -9)
30 plt.grid()
31 plt.show()
32 #Plots the galactic coordinates of the given data.

```

Listing 4: Now we are going to plot the spectra labeling the max (red) and peak (blue) velocities. Running this repeatedly will overwrite previous diagrams with same name. The spectra are saved to a folder called 'plots' which will be created if it does not already exist.

```

1 def plot_spectrum(filename, peak_threshold=0.2):
2
3     # Load spectrum data from file
4     vel, P = np.loadtxt('data/{}'.format(filename), skiprows=8, unpack=
5         True)
6
7     # Find the peak velocities and intensities
8     max_intensity = np.max(P)
9     peak_indices = np.where(P >= 0.8 * max_intensity)[0]
10    peak_velocities = vel[peak_indices]
11    peak_intensities = P[peak_indices]
12
13    # Find the velocity of the peak with the greatest x value
14    peak_index = np.argmax(peak_velocities)
15    peak_velocity = peak_velocities[peak_index]
16    peak_intensity = peak_intensities[peak_index]
17
18    # Find the velocity corresponding to the specified threshold intensity
19    threshold_intensity = peak_threshold * peak_intensity
20    threshold_index = np.argmin(np.abs(P[:peak_indices[peak_index]] -
21        threshold_intensity))
22    threshold_velocity = vel[threshold_index]

```

```

22 # Plot the data and vertical lines
23 fig, ax1 = plt.subplots()
24 ax1.set_xlabel(r"Velocity (km\s$^{-1}$)")
25 ax1.set_ylabel(r"Intensity (counts)")
26 ax1.ticklabel_format(axis='x', style='plain')
27 ax1.plot(vel, P, linestyle='--', color='k')
28
29 mlinex = [peak_velocity, peak_velocity]
30 mliney = [0, peak_intensity + 10]
31 plinex = [threshold_velocity, threshold_velocity]
32 pliney = [0, peak_intensity + 10]
33 ax1.plot(mlinex, mliney, linestyle='dotted', color='red')
34 ax1.plot(plinex, pliney, linestyle='dotted', color='blue')
35
36 GLON_GLON = filename[:-4].split('_')
37 GLON_file = float(GLON_GLON[0])
38
39 with open(fileSM, "a") as f1, open(fileSP, "a") as f2:
40     f1.write('{}\n'.format(GLON_file, threshold_velocity))
41     f2.write('{}\n'.format(GLON_file, peak_velocity))
42
43 plt.tight_layout()
44 plt.title('({}_GLON) = ' + filename[:-4])
45 plt.grid()
46 plt.savefig('plots/{}.png'.format(filename[:-4]))
47 plt.close()
48
49 #Define the directory path where the files are located
50 directory = 'data'
51
52 #Get a list of all the files in the directory
53 files = os.listdir(directory)
54
55 # Create the 'plots' directory if it doesn't exist
56 os.makedirs('plots', exist_ok=True)
57
58 for f in files:
59     plot_spectrum(f, 0.5)

```

Listing 5: Process the example data and collected data.

```

1 #Model from (McGaugh, 2018, RNAAS, 2, 156).
2 Rm,Vbm,Vgm,Vkm,Vdm,Vm,Vcm = np.loadtxt("processed/McGaugh_model.txt",
3     skiprows=3, unpack = True)
4 #Data from (McClure-Griffiths & Dickey, 2007, ApJ, 671, 427).
5 Rc,Vc = np.loadtxt("processed/McClure07.txt", skiprows=3, unpack = True)
6 #Our SALSA data (measured at edge of largest velocity).
7 glonM,VOM = np.loadtxt("processed/salsa_max.txt", unpack = True)
8 #Our SALSA data (measured at highest peak in velocity).
9 glonP,VOP = np.loadtxt("processed/salsa_peak.txt", unpack = True)

```

Listing 6: Solar Values.

```

1 vsun = 220 # km/s (Salsa)
2 rsun = 8.5 # kpc (Salsa)
3 ##vsun = 233 # km/s (McGaugh)
4 ##rsun = 8.12 # kpc (McGaugh)

```

```

5
6 vsinl = vsun * np.sin( glonM * np.pi / 180.)
7 rsinl = rsun * np.sin( glonM * np.pi / 180.)
8 rcosl = rsun * np.cos( glonM * np.pi / 180.)

```

Listing 7: Estimate errors and calculate rotational velocities.

```

1 vread = 5 # km/s (assumed error in velocity calculation)
2
3 vrotM = VOM + vsinl # edge of largest velocity
4 vrotP = VOP + vsinl # highest peak in velocity

```

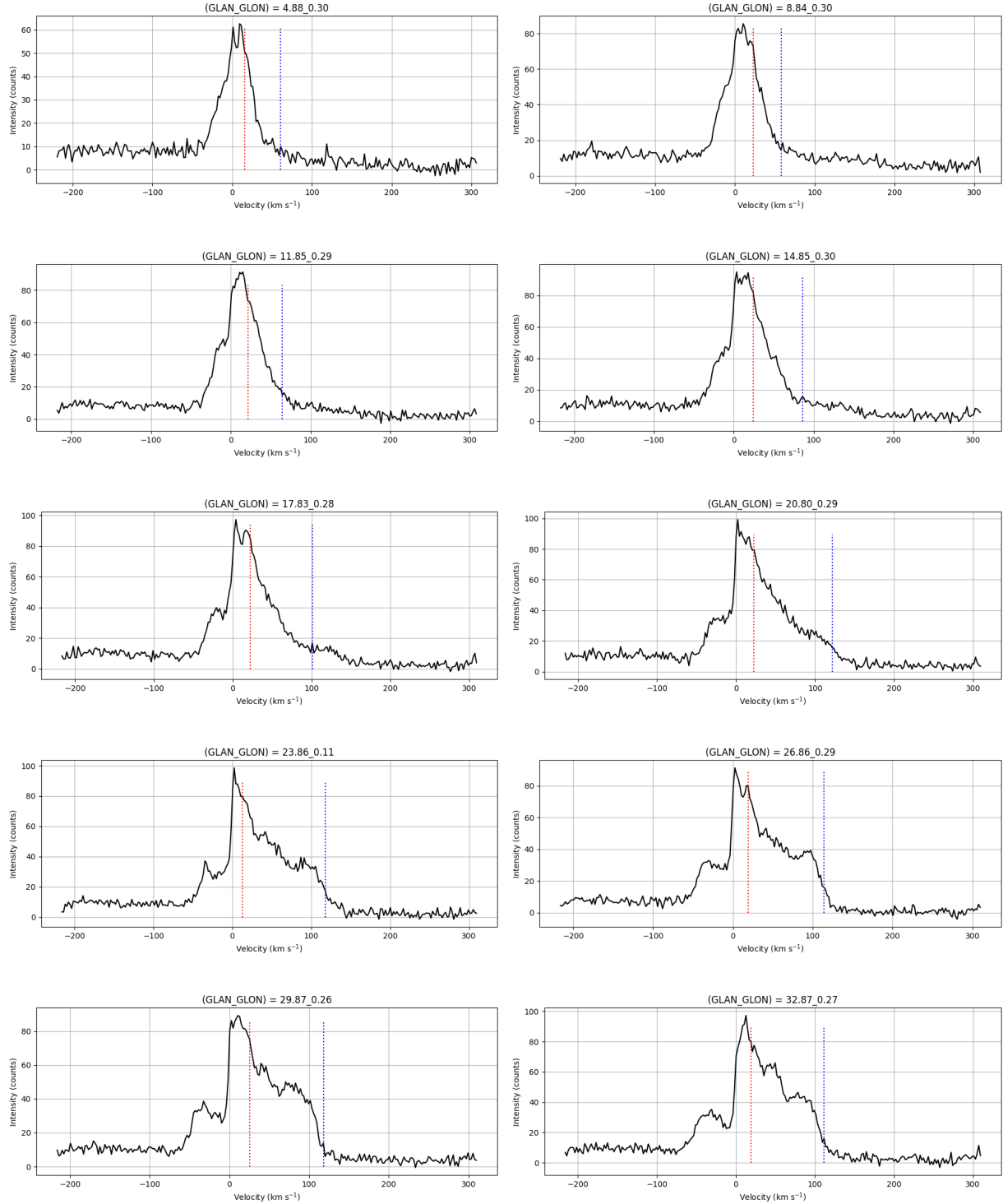
Listing 8: Plot rotation curve.

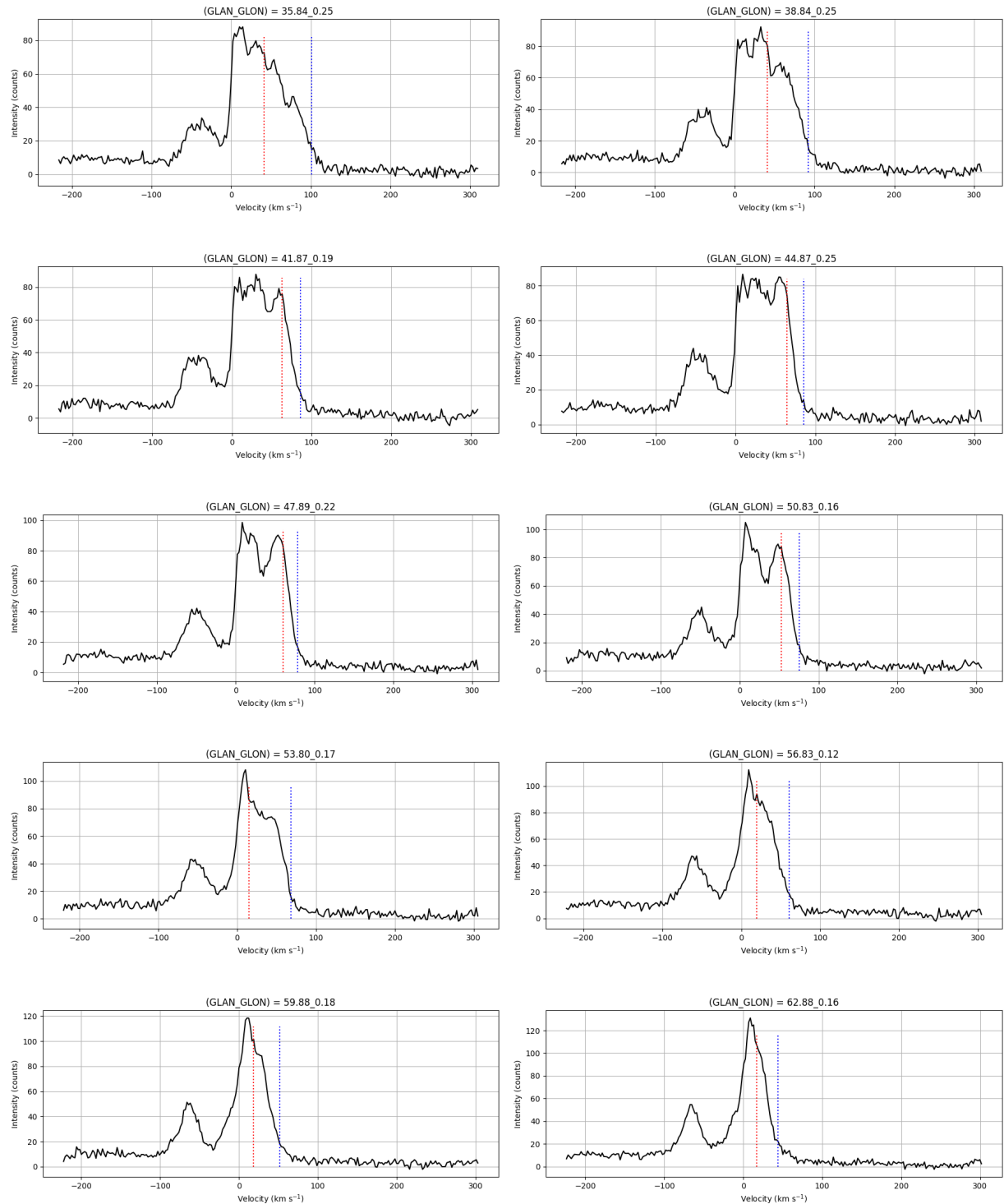
```

1 fig, ax1 = plt.subplots()
2 ax1.set_xlabel(r"Radius□(kpc)")
3 ax1.set_ylabel(r"V□(km/s)")
4 ax1.set_xlim(0, 10)
5 ax1.set_ylim(100, 270)
6 ax1.ticklabel_format(axis='x', style='plain')
7 ax1.plot(Rm,Vm, linestyle='--', color='k') ## total McGaugh model
8 ax1.plot(Rc,Vc, linestyle='--', color='red') ## McClure data
9 ax1.errorbar(rsinl,vrotM, yerr=vread, fmt='o', color='navy')
10 ax1.errorbar(rsinl,vrotP, yerr=vread, fmt='o', fillstyle='none', color='coral')
11 plt.tight_layout()
12 plt.grid()
13 plt.savefig('Rotation_Curve.png')

```

B Appendix - Graphs





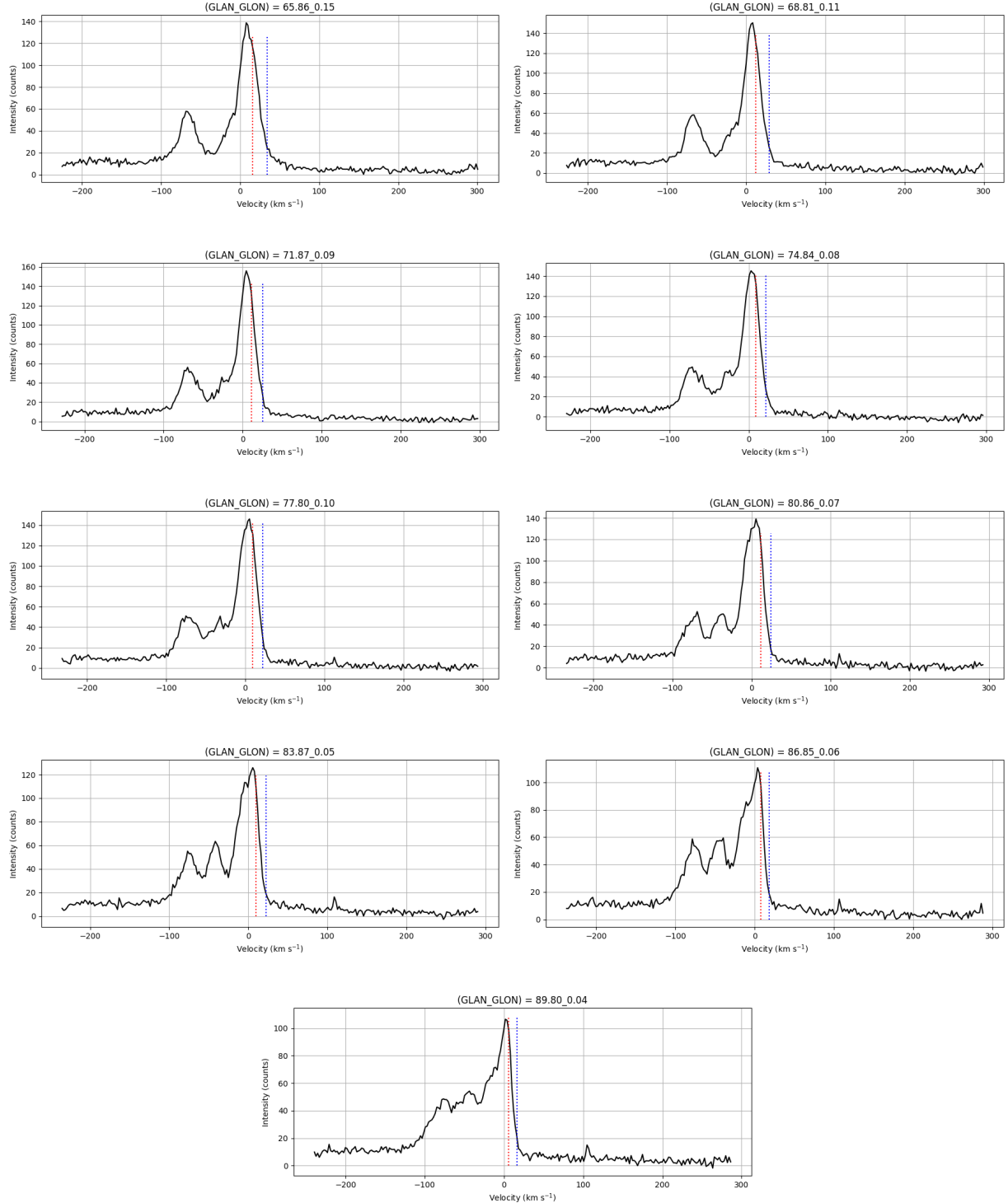


Figure 16: Plotted spectra of various galactic longitudes. Each graph has an orange and blue dotted line representing the peak and max velocity values respectively.